Energy 66 (2014) 965–972

Contents lists available at ScienceDirect

Energy

journal homepage: www.elsevier.com/locate/energy

Thermoelectric power generation driven by blast furnace slag flushing water

Fankai Meng [a,b,c], Lingen Chen [a,b,c,*], Fengrui Sun [a,b,c], Bo Yang [a,b,c]

[a] Institute of Thermal Science and Power Engineering, Naval University of Engineering, Wuhan 430033, China
[b] Military Key Laboratory for Naval Ship Power Engineering, Naval University of Engineering, Wuhan 430033, China
[c] College of Power Engineering, Naval University of Engineering, Wuhan 430033, China

ARTICLE INFO

Article history:
Received 25 July 2013
Received in revised form
3 February 2014
Accepted 4 February 2014
Available online 26 February 2014

Keywords:
Iron and steel industry
Slag flashing water
Waste heat recovery
Energy-saving
Thermoelectric
Power generation

ABSTRACT

Focusing on the low recycling rate of low temperature waste heat in China's iron and steel industry, this study presented a technical solution recycling blast furnace slag flashing water sensible heat based on thermoelectric power generation. The physical and numerical models are established. The effects of some key parameters such as slag washing water temperature, the thermoelectric element length, the packing factor of the thermoelectric module and heat exchanger flow passage length on the performance of the thermoelectric power generation device are analyzed. The results showed that for blast furnace slag flushing water at 100 °C, water temperature drops 1.5 °C per meter, about 0.93 kW electrical energy can be produced per area and conversion efficiency of 2% can be achieved. The cost recovery period of the equipment is about 8 years.

1. Introduction

The energy consumption has become one of the main problems which restricts the sustainable development of China. The recovery and utilization of different kinds of waste heat can effectively reduce energy consumption. The research of the recovery and utilization of waste heat becomes very important [1–4].

Iron and steel industry waste heat is rich, variety and in a wide temperature range. Taking advantage of these waste heat is of great significance for reducing energy consumption and emissions [5]. According to the statistics of China's iron and steel enterprises, the average recovery of waste heat resources is only 25.8% while low temperature waste heat recovery rate is less than 1%.

Power generation is the highest value utilization among various waste heat utilization forms. However, the lower waste heat temperature, the lower efficiency of power recovery and the greater difficulty from a technical perspective. Conventional steam turbine power generation system cannot be used for low temperature waste heat power recovery [6]. For the blast furnace, converter and electric furnace slag sensible heat, only water quenching method recovering hot water has been applied while the others are still in the experimental research stage [7]. Using the flashing water sensible heat to heat the residents in winter is the main utilization way in China. This simple and low-cost way has been widely used but has two problems: first, slag water contains a great deal of heat but the heating load is small usually. Second, heating is only applicable in northern China cities in winter while the southern cities and summer have no such needs [8].

Thermoelectric power generation is one of the three most potential power generation technologies in the 21st century. In recent years, with improved conversion efficiency and dropped cost of thermoelectric materials, thermoelectric power generation technology has moved from the aerospace, military and other frontiers toward the industrial and people's life. In the field of low-grade waste heat utilization, thermoelectric power generation technology can compete with conventional power generation technologies and become the main way of low-grade thermal power generation gradually [9].

According to the market statistics, in the field of thermoelectric materials consumption, low-grade thermoelectric power generation accounts for 30% market share, which exceeds cooling and heating. Thermoelectric-based power generation technology recycling industrial waste heat has become one of the research hotspots in the energy saving field. Suzuki and Tanaka [10–13] designed a series of thermoelectric generators and deduced analytical

* Corresponding author. College of Power Engineering, Naval University of Engineering, Wuhan 430033, China. Tel.: +86 27 83615046; fax: +86 27 83638709.
E-mail addresses: lgchenna@yahoo.com, lingenchen@hotmail.com (L. Chen).

http://dx.doi.org/10.1016/j.energy.2014.02.018
0360-5442/

Nomenclature

A	area (m^2)
B	flow channel width (m)
c	specific heat capacity at constant pressure ($J\ kg^{-1}\ K^{-1}$)
G	mass flow rate ($kg\ s^{-1}$)
h	convective heat transfer coefficient ($W\ m^2\ K^{-1}$)
I	electrical current (A)
K	thermal conductance ($W\ K^{-1}$)
L	length (m)
N	number
P	power output (W)
p	power-per-area ($W\ m^{-2}$)
Q	heat flow rate (W)
R	electrical resistance (Ω); thermal resistance ($m^2\ K\ W^{-1}$)
T	thermodynamic temperature (K)
t	Celsius temperature (°C)
u	velocity ($m\ s^{-1}$)

Greek letters

α	Seebeck coefficient ($V\ K^{-1}$)
σ	electrical conductivity ($\Omega^{-1}\ m^{-1}$)
λ	thermal conductivity ($W\ m^{-1}\ K^{-1}$)
θ	packing factor
η	conversion efficiency

Subscripts

1	hot fluid
2	cold fluid
c	cold junction
cp	ceramic substrate of thermoelectric module
ex	heat exchanger
f	flow channel
g	air gap
h	hot junction
L	load
n	N-type semiconductor leg
p	P-type semiconductor leg

expressions of electric power in case of the cylindrical thermoelectric tubes, flat thermoelectric panels, cylindrical double tubes, multiple cylindrical tubes exposed to two thermal fluids. Their research has important significance for large-scale thermoelectric power generation. Yu and Zhao [14] presented a numerical model to predict the performance of thermoelectric generator with the parallel-plate heat exchanger. The simulation results showed that the variations in temperature of the fluids in the thermoelectric generator are linear. Niu et al. [15] constructed an experimental thermoelectric generator unit incorporating the commercially available thermoelectric modules with the parallel-plate heat exchanger. They found that the hot fluid inlet temperature and mass flow rate significantly affect the maximum power output and conversion efficiency. Astrain et al. [16] calculated the efficiency of a thermoelectric generation using the heat of the smoke from a paper mill's combustion boiler as heat source. The results demonstrated that it was possible to generate about 1 kW per meter of chimney height, that is, about 300 W/m^2. Meng et al. [17] established a numerical model of commercial thermoelectric module with finned heat exchangers. Hot water at 60–100 °C and cold water at 27 °C were employed as heat source and sink of the generator module. The results showed that the maximum power output of 0.13 W and the maximum efficiency of 0.87% were available from a module. Jang et al. [18] investigated the power output performance of the TEG module which embedded in the chimney walls. The three-dimensional turbulent flow in a chimney used for venting flue gas from either a boiler or stove was analyzed. Lu et al. [19] tried to conceptually combine exhaust heat exchanger with muffler in the form of 1-inlet and 2-outlet, 2-inlet and 2-outlet as well as the baseline empty cavity. The test results showed that 1-inlet and 2-outlet increased hydraulic disturbance and enhanced heat transfer, resulting in the more uniform flow distribution and higher surface temperature than the others.

On the basis of research achievements mentioned above, this paper presents a thermoelectric power generation technology-based blast furnace slag flushing water waste heat recovery solution. The physical model is established and numerical examples are provided to analyze the key design parameters of the device. Finally, economic analysis is performed adopting commercial thermoelectric module specifications. The results may provide some guidelines for the applications of thermoelectric power generation technology in industrial waste heat recovery.

2. Flushing slag water driven thermoelectric power generation device and the physical model

Flushing slag water is continuous fluid form of waste heat. The heat transfer and energy conversion of recycling process based on thermoelectric power generation technology can be described as: the hot fluid (blast furnace slag water) temperature decreases gradually along the flow. Meanwhile, part of the heat rejected is taken away by the cold fluid (cooling water at room temperature); the other part of the heat is recovered by the thermoelectric power generation modules and converted to electrical energy.

The blast furnace slag water waste heat recovery system based on thermoelectric power generation technology is shown in Fig. 1. It is mainly composed of two parts. One is the thermoelectric power generating module which can convert thermal energy to electrical energy. Another is the heat exchanger between thermoelectric modules and waters. The structure of the flow channel cross-section of the plate–fin heat exchanger is shown in Fig. 2. A P-type and an N-type semiconductor leg compose a thermoelectric element. Due to the insulation requirements and process limitations, thermoelectric elements cannot be closely arranged and then a air gap exists inside the module. This causes part of the heat flows through the air gap directly (gray arrows in Fig. 1).

The physical model of the flushing slag water driven thermoelectric power generation device is shown in Fig. 3. This model

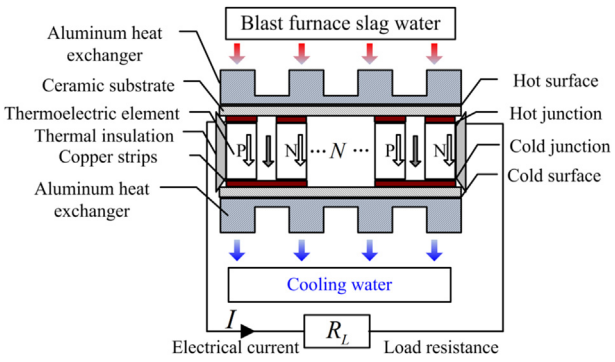

Fig. 1. Schematic diagram of the blast furnace slag water heat recovery device based on thermoelectric power generation technology.

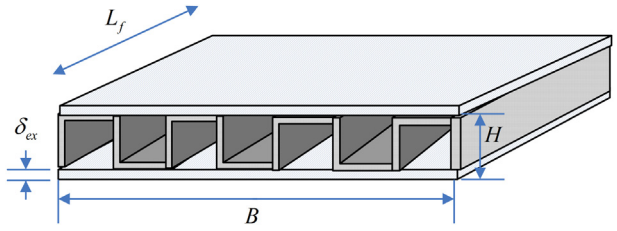

Fig. 2. Structure of the fluid heat transfer passage.

draws on the Yu and Zhao's method [14], but makes some improvements. First, the gap between the thermoelectric elements and the loss of heat leakage are considered which makes the results more accurate. Module air gap is described with a coefficient called packing factor which has significant impact on the power density of the module [20]. Second, the model contains the thermoelectric element length which provides the foundation for geometry optimization.

The flushing slag water and cooling water temperatures are $T_1(x)$ and $T_2(x)$, respectively. Thermoelectric element hot and cold junction temperatures are $T_h(x)$ and $T_c(x)$, respectively. Thermoelectric element length and cross-sectional area are L and A, respectively. The thermoelectric module ceramic substrate thickness and packing factor are δ_{cp} and θ $(0 < \theta \leq 1)$ respectively. Packing factor is defined as

$$\theta = 2AN/A_{cp} \tag{1}$$

Slag flushing water discharged and cooling water absorbed heat flow rates are Q_1 and Q_2, respectively. The thermoelectric module absorbed and discharged heat flow rates are Q_h and Q_c, respectively. The load resistance and electrical current output of the generator are R_L and I, respectively. The heat exchanger separator thickness is δ_{ex}. The height, width, and length of the flow channel are H, B and L_f, respectively. The slag flushing water and cooling water inlet temperatures are T_{10} and T_{20}, respectively. The mass flow rates of water are G_1 and G_2, respectively. The specific heat capacities are c_{p1} and c_{p2}, respectively. The thermal resistances of the ceramic substrate, heat exchanger separator, convective heat transfer (for the first order heat transfer surface) and air gap (thermal conduction) are given by

$$R_{cp} = \delta_{cp}/\lambda_{cp} \tag{2}$$

$$R_{ex} = \delta_{ex}/\lambda_{ex} \tag{3}$$

$$R_{cv} = 1/h \tag{4}$$

$$R_g = L/\lambda_{air} \tag{5}$$

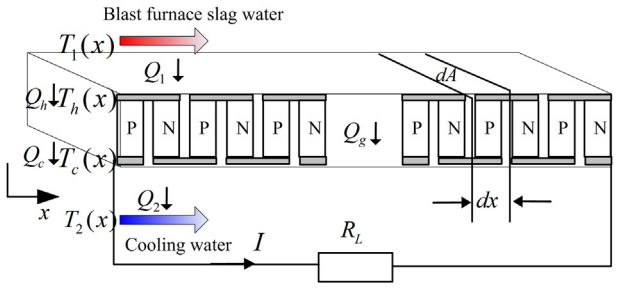

Fig. 3. Physical model of the power generation device.

Taking infinitesimal volume as shown in Fig. 3, according to the theory of heat transfer and non-equilibrium thermodynamics [21], one can obtain

$$dQ_1 = -G_1 c_{p1} dT_1(x) \tag{6}$$

$$dQ_1 = K_1[T_1(x) - T_h(x)]B\,dx \tag{7}$$

$$dQ_h = \left[\alpha T_h(x)I + K(T_h(x) - T_c(x)) - \frac{I^2R}{2}\right]\frac{\theta B\,dx}{2A} \tag{8}$$

$$dQ_g = K_g[T_h(x) - T_c(x)](1-\theta)B\,dx \tag{9}$$

$$dQ_c = \left[\alpha T_c(x)I + K(T_h(x) - T_c(x)) + \frac{I^2R}{2}\right]\frac{\theta B\,dx}{2A} \tag{10}$$

$$dQ_2 = G_2 c_{p2} dT_2(x) \tag{11}$$

$$dQ_2 = K_2[T_c(x) - T_2(x)]B\,dx \tag{12}$$

The system heat balance equations are given by

$$Q_1 = Q_h + Q_g \tag{13}$$

$$Q_2 = Q_c + Q_g \tag{14}$$

Eqs. (6)–(12) can be organized into differential equations about $T_1(x)$, $T_h(x)$, $T_c(x)$, $T_2(x)$ as follows

$$T_1'(x) = \frac{K_1[T_1(x) - T_h(x)]B}{-G_1 c_{p1}} \tag{15}$$

$$K_1(T_1(x) - T_h(x)) = \left[\alpha T_h(x)I + K(T_h(x) - T_c(x)) - \frac{I^2R}{2}\right]\frac{\theta}{2A} + K_g(T_h(x) - T_c(x))\frac{1-\theta}{L} \tag{16}$$

$$K_2(T_c(x) - T_2(x)) = \left[\alpha T_c(x)I + K(T_h(x) - T_c(x)) + \frac{I^2R}{2}\right]\frac{\theta}{2A} + K_g(T_h(x) - T_c(x))\frac{1-\theta}{L} \tag{17}$$

$$T_2'(x) = \frac{K_2[T_c(x) - T_2(x)]B}{-G_2 c_{p2}} \tag{18}$$

The temperature boundary conditions are (assuming that the flow is parallel flow)

$$T_1(0) = T_{10} \tag{19}$$

$$T_2(0) = T_{20} \tag{20}$$

where α, K and R are the total Seebeck coefficient, thermal conductance and electrical resistance of a thermoelectric element, respectively. They can be calculated by

$$\alpha = \alpha_p - \alpha_n \approx 2\alpha_p \tag{21}$$

$$K = K_p + K_n = \lambda_p A_p/L_p + \lambda_n A_n/L_n \approx 2\lambda_p A/L \tag{22}$$

$$R = R_p + R_n = L_p/(\sigma_p A_p) + L_n/(\sigma_n A_n) \approx 2L/(\sigma_p A) \quad (23)$$

where λ and σ are the thermal and electrical conductivities of the thermoelectric element.

The power output from the device is the slag flushing water released heat minus the cooling water absorbed heat, which is given by

$$P = G_1 c_{p1}\left[T_1(0) - T_1\left(L_f\right)\right] - G_2 c_{p2}\left[T_2\left(L_f\right) - T_2(0)\right] \quad (24)$$

The conversion efficiency of the device is power output divided by the heat slag flushing water released, which is given by

$$\eta = 1 - \frac{G_2 c_{p2}\left[T_2\left(L_f\right) - T_2(0)\right]}{G_1 c_{p1}\left[T_1(0) - T_1\left(L_f\right)\right]} \quad (25)$$

Because the device employs the iron and steel industry waste heat as heat source, power rather than efficiency is the primary optimization criterion. Some studies [22,23] indicated that the power output reaches the maximum when the load resistance equals to the thermoelectric generator internal resistance. The power in the numerical calculation below refers to the maximum power when the load resistance equals the internal resistance while the efficiency refers to the efficiency corresponding to the maximum power. As the model uses electrical current as variable, iterative calculation method needs to be adopted. Relation between current and load resistance is given by

$$I = \sqrt{\frac{P}{R_L}} \quad (26)$$

3. Numerical simulation and economic analysis

The effects of the key parameters on the device performance are analyzed from inside to outside by numerical calculations. As the slag flushing water temperature is less than 100 °C, the most appropriate thermoelectric materials corresponding the temperature range is bismuth telluride (Bi_2Te_3) semiconductor thermoelectric materials. Considering the slag flushing water temperature range is small, this study does not take the material properties variation into account. The physical parameters of the commercially available material by Melcor at 60 °C are used for this simulation. The parameters set are listed in Table 1.

3.1. Effect of thermoelectric element length

Figs. 4 and 5 show the power and efficiency versus thermoelectric length at different slag washing water inlet temperature t_1. $\theta = 0.5$, $h = 3000$ W m^{-2} K^{-1}, $B = 0.1$ m, $H = 6$ mm, and $L_f = 10$ m are set in the calculation. It can be seen that there is an optimal thermoelectric element length corresponding to the maximum power. The power and the corresponding optimum thermoelectric element length increases simultaneously with the slag flushing water temperature. In general, commercial thermoelectric module

Table 1
Parameters set in the numerical simulation.

α (10^{-4} V K^{-1})	λ (W m^{-1} K^{-1})	σ (10^5 m Ω^{-1})	A (mm^2)	δ_{cp} (mm)
4.4	1.5	1	1 × 1	1
λ_{cp} (W K^{-1} m^{-1})	c_p (10^3 J kg^{-1} K^{-1})	λ_{ex} (W K^{-1} m^{-1})	δ_{ex} (mm)	u (m s^{-1})
35.3	4.2	204	2	1

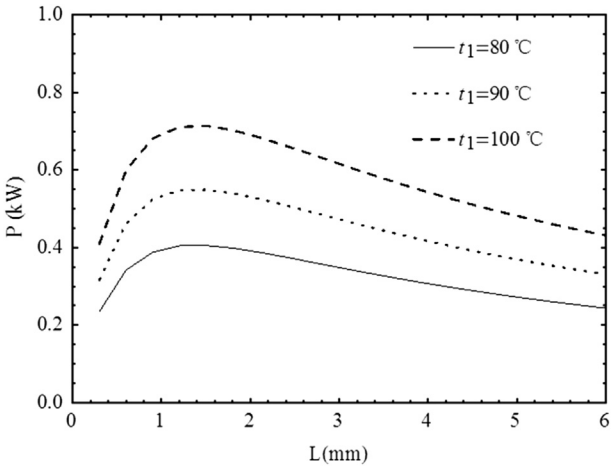

Fig. 4. Power versus thermoelectric length at different slag washing water inlet temperature.

hot surface maximum operating temperature is below 180 °C and the thermoelectric element length is 1.0–2.0 mm. The optimum thermoelectric element length calculated in this simulation is approximately 1.2 mm, which shows that common commercial thermoelectric module size basically meets the slag flushing water power generation requirements without customization of special size thermoelectric modules. Efficiency increases with the increases of thermoelectric element length and slag flushing water temperature. The efficiency corresponding to the maximum power is 1.6–1.8%.

Figs. 6 and 7 show the effects of convective heat transfer coefficient h on power and efficiency versus thermoelectric length. $\theta = 0.5$, $B = 0.1$ m, $H = 6$ mm, $L_f = 10$ m and $t_1 = 100$ °C are fixed in the calculation. It can be seen that the maximum power and efficiency increase when the convective heat transfer coefficient increases. The optimal length of the thermoelectric element corresponding to the maximum power decreases. This shows that the enhancement of heat transfer between water and heat exchangers can effectively improve the power and efficiency. In fact, this is because the external thermal resistance and the heat loss is reduced, which increase the temperature difference between the

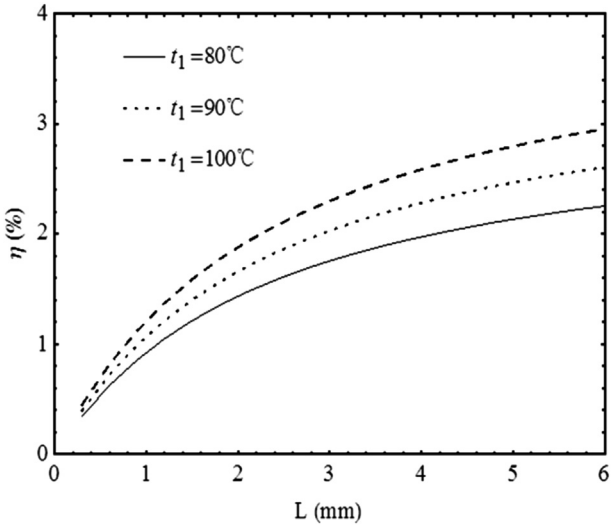

Fig. 5. Efficiency versus thermoelectric length at different slag washing water inlet temperature.

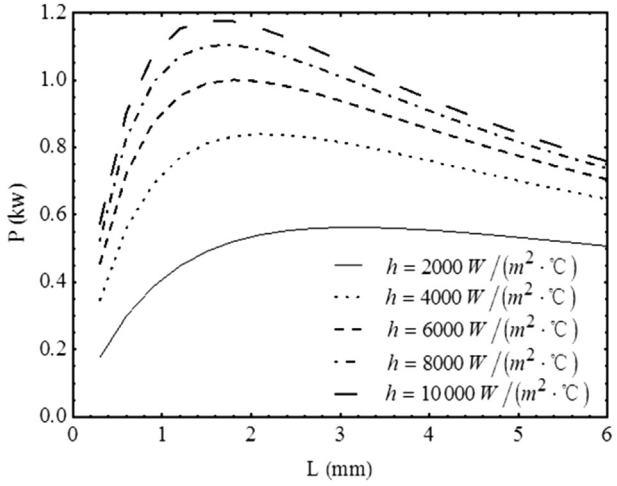

Fig. 6. Effect of convective heat transfer coefficient on power versus thermoelectric element length.

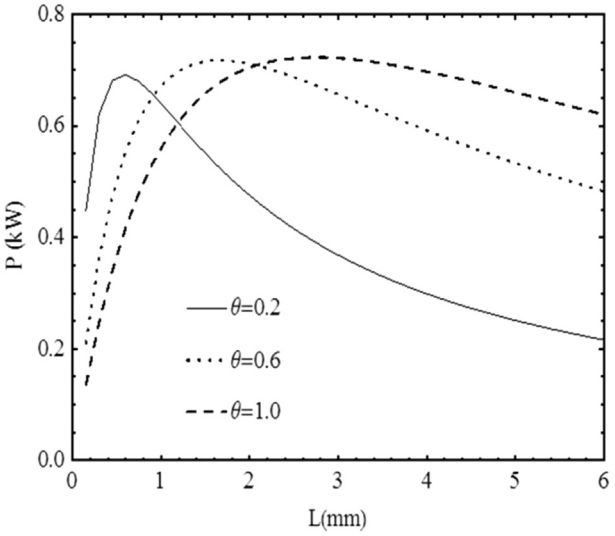

Fig. 8. Effect of packing factor on power versus thermoelectric element length.

junctions of the thermoelectric elements. When the external thermal resistance tends to zero, the temperature difference between the hot and cold junctions tends to the temperature difference between the slag flushing water and the cooling water, and then the power and efficiency tend to the maximum accordingly. For plate–fin heat exchanger, the water–water convective heat transfer coefficient is 3000–5000 W m^{-2} K^{-1}, so the corresponding power and efficiency are 0.8 kW and 1.8% approximately, respectively.

3.2. Effect of thermoelectric module packing factor

Figs. 8 and 9 show the effects of module packing factor θ on power and efficiency versus thermoelectric length. $h = 3000$ W m^{-2} K^{-1}, $B = 0.1$ m, $H = 6$ mm, $L_f = 10$ m and $t_1 = 100$ °C are fixed in the calculation. It can be seen that the optimal thermoelectric element length increases with the increase of packing factor. The power reaches the maximum when the thermoelectric element length matches the packing factor. Increasing the packing factor does not significantly enhance the performance, because not only the maximum power changed little, but also the efficiency decreases. Therefore, thermoelectric modules do not require a dense arrangement of thermoelectric elements, because it will not only increase the cost of equipment, but also reduces the temperature difference between the surfaces of the thermoelectric module, thereby reduces the efficiency of the device.

Figs. 10 and 11 show the effects of slag washing water inlet temperature t_1 on power and efficiency versus module packing factor. $h = 3000$ W m^{-2} K^{-1}, $B = 0.1$ m, $H = 6$ mm, and $L = 2$ mm are fixed in the calculation. It can be seen that for given slag flushing water temperature and cooling water temperature, when the packing factor increases, the power first increases and then decreases, but there was little change. Due to the constant cross-sectional area of the thermoelectric elements, on the one hand, increase the packing factor will increase the number of the thermoelectric element, which improves the total power; on the other hand, the total thermal resistance and then the temperature difference of the thermoelectric module are reduced, which decreases the power generated from a single thermoelectric element. When the effects of both are balanced, power reaches the maximum.

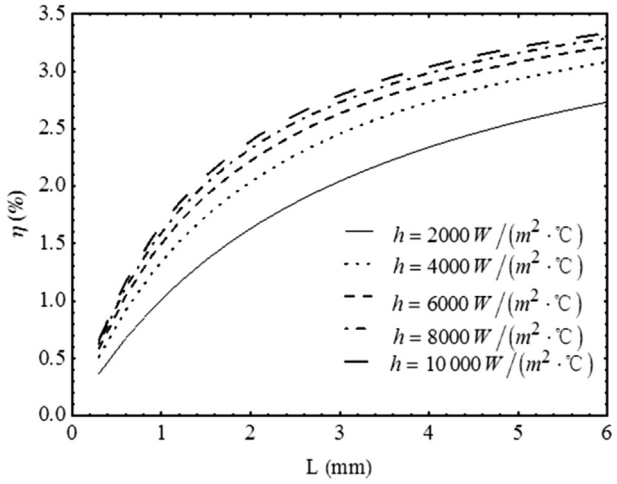

Fig. 7. Effect of convective heat transfer coefficient on efficiency versus thermoelectric element length.

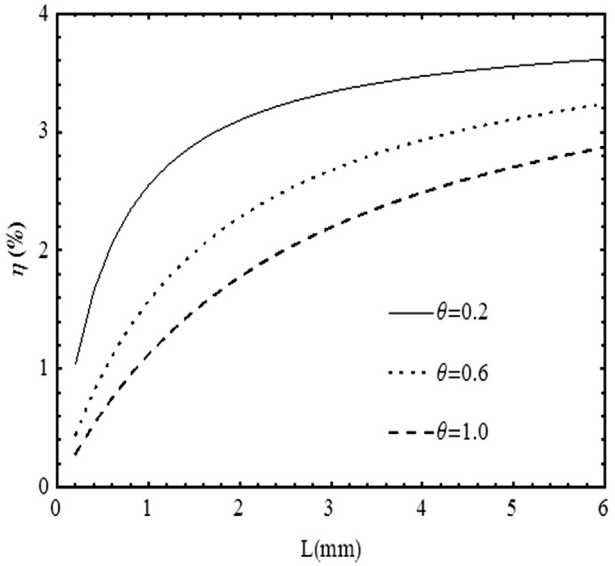

Fig. 9. Effect of packing factor on efficiency versus thermoelectric element length.

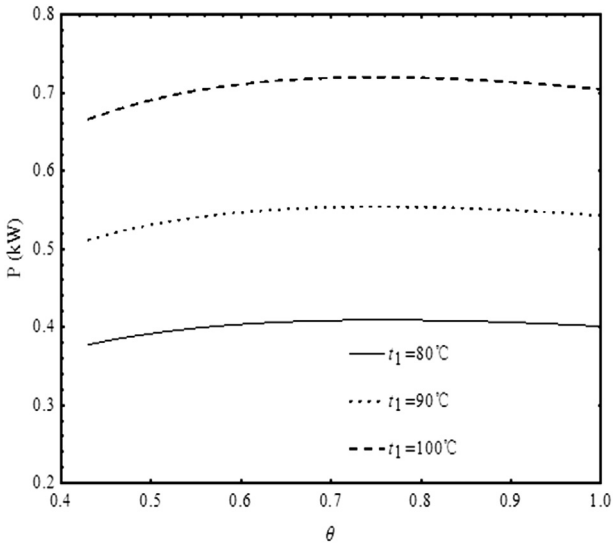

Fig. 10. Effect of flushing slag water temperature on power versus packing factor.

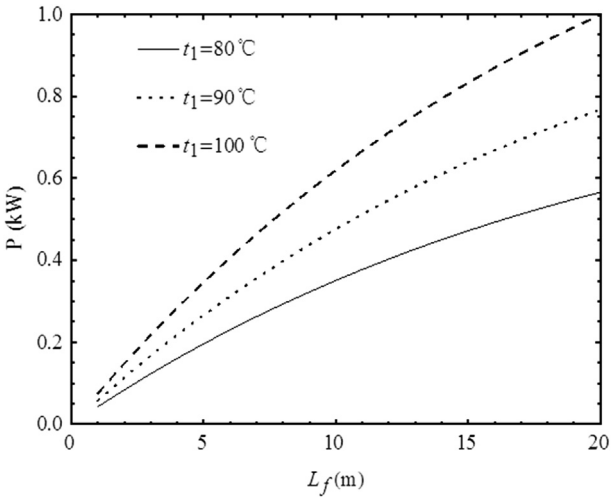

Fig. 12. Power versus flow passage length.

The flow channel size is kept constant in the above analyses and the total heat transfer area is $A_h = B \times L_f = 1\ m^2$. Therefore, the power is also the power-per-area.

3.3. Effect of fluid channel length

Figs. 12 and 13 show the power and efficiency versus fluid channel length. $\theta = 0.5$, $h = 3000\ W\ m^{-2}\ K^{-1}$, $B = 0.1$ m, $H = 6$ mm and $L = 2$ mm are fixed in the calculation. The figures show that the power increases with flow path length non-linearly and the growth rate decreases. Efficiency decreases with the length of the flow path non-linearly. The reason of nonlinearity is that the slag flushing water temperature reduced gradually which leading to the decrease of thermoelectric modules temperature difference.

Fig. 14 shows slag flushing water temperature t_1, cooling water temperature t_2, the hot junction temperature t_h and cold junction temperature t_c versus fluid channel length. Fig. 15 shows the power-per-area p versus fluid channel length. $\theta = 0.5$, $h = 3000\ W\ m^{-2}\ K^{-1}$, $B = 0.1$ m, $H = 6$ mm, $L = 2$ mm and $t_{10} = 100\ ^\circ C$ are fixed in the calculation. It can be seen that the temperature change is non-linear which is different from the result obtained by Yu and Zhao [14]. The reason for this may be the flow channel length in their calculation is too short to see the non-linear characteristics. The second reason may be this model takes into account the heat leakage through the air gap which affects the temperature distribution. The numerical results show that slag flashing water temperature drops about 1.5 °C per meter of the flow channel. When the flow channel length reaches 20 m, the thermoelectric module temperature difference is less than 10 °C at the outlet.

The lower slag flashing water outlet temperature means the more fully utilized of waste heat. However, from the economic point of consideration, the length of the flow channel should not be too long; otherwise the module average temperature difference is too small which leading to the too low overall efficiency of the device. The total power requirements of the device can be achieved in two ways. One option is to increase the number of heat exchanger channels. Each fluid channel constitutes a basic unit so they can be easily combined. Another option is to increase the width of the heat exchanger channel. The calculations show that the total power output is proportional to the channel width and the number of channels.

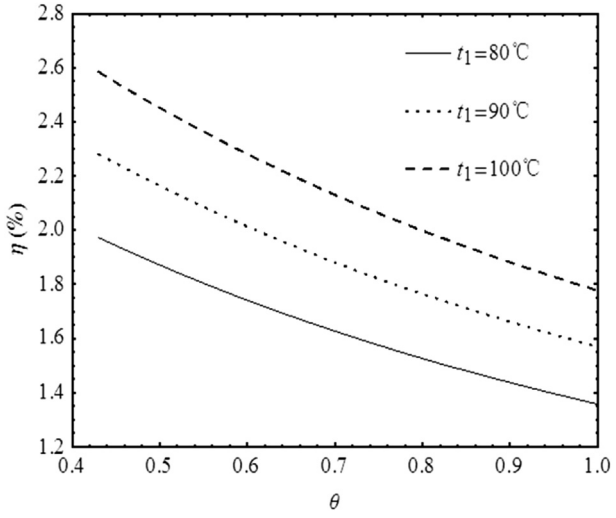

Fig. 11. Effect of flushing slag water temperature on efficiency versus packing factor.

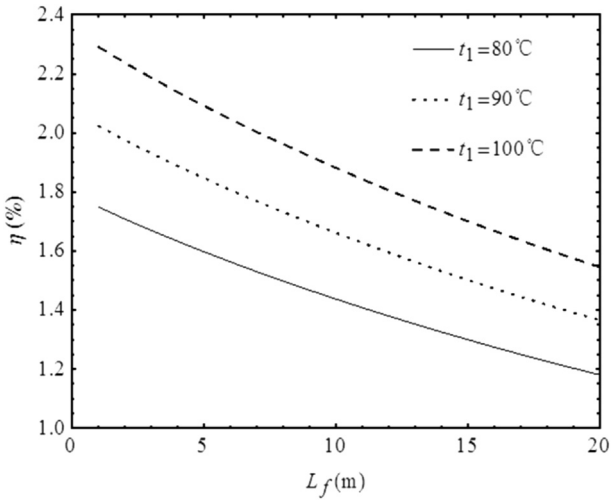

Fig. 13. Efficiency versus flow passage length.

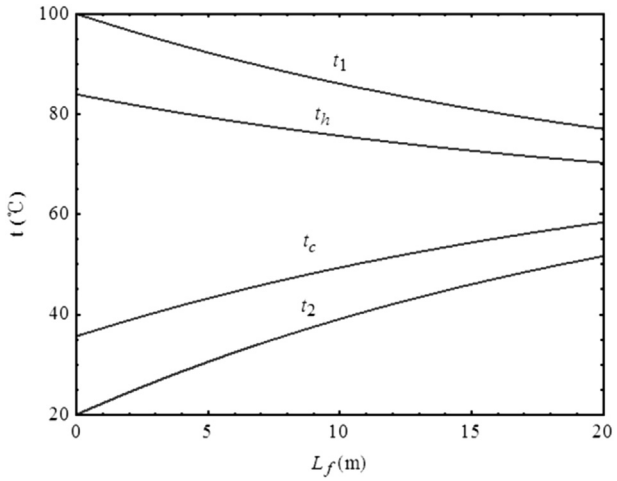

Fig. 14. Temperatures versus flow passage length.

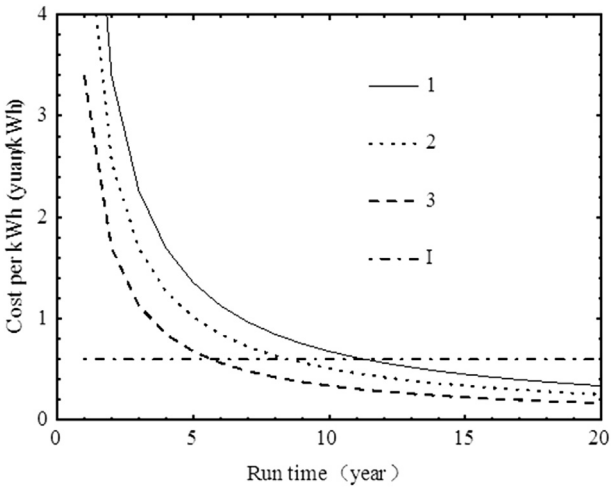

Fig. 16. Cost per kWh versus run time.

3.4. Economic analysis

Parameters of commercial thermoelectric module are adopted to analyze the economy of slag flushing water driven thermoelectric power generation technology. In general, the cost of a thermoelectric power generator essentially consists of the device cost and the operating cost. Considering the high reliability of thermoelectric device, the operation and maintenance cost is not much in the entire operation cycle [24]. For large-scale thermoelectric power generation equipment, the major cost of the total device is consumed by thermoelectric modules (the greater total power output, the smaller proportion of costs of accessory equipment) [25]. On the other hand, depreciation, repair and accessory equipments such as piping are not suitable for calculation by cost-per-watt, so they are not included into the total cost in this analysis. Nonetheless, the payback period estimations are still credible.

The generation module specifications are as follows: $A_m = 40 \times 40$ mm^2, $A = 1.2 \times 1.2$ mm^2, $L = 2$ mm and $N = 127$. The packing factor can be calculated as $\theta = 0.4$. The convective heat transfer coefficient is set as $h = 3000$ W m^{-2} K^{-1}. It can be calculated that 0.93 kW electric power can be generated per square meter. Fig. 16 shows the cost per kWh versus operation time of the power generation device. The curves 1, 2 and 3 represent thermoelectric module prices of 40 yuan, 30 yuan, and 20 yuan, respectively. Curve I represents market industrial electricity price of 0.6 yuan/(kWh) in China. The figure shows that the cost per kWh decreases gradually with the device operating time. When the average cost is lower than the market electricity price, the device begins to profit. The device payback periods corresponding to different thermoelectric module prices are approximately 11 years, 8 years and 6 years, respectively. With the declining price of thermoelectric materials and advances in modules manufacturing technology, the payback period is expected to be further reduced.

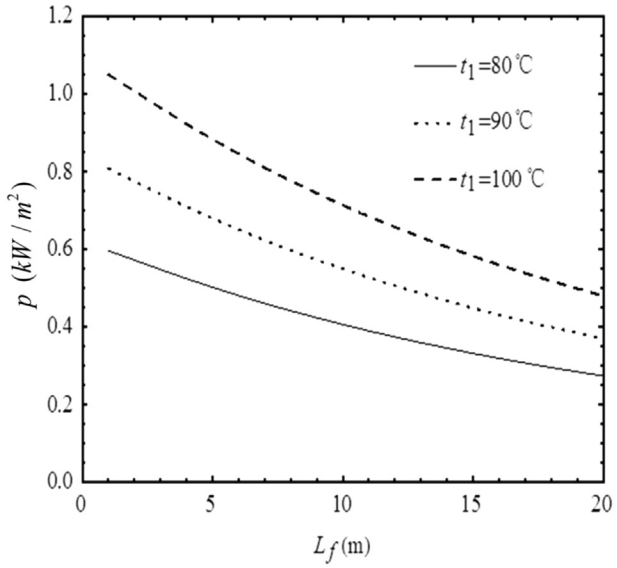

Fig. 15. Power-per-area versus flow passage length.

4. Discussions

The temperature of slag from blast furnace, converter, and electric furnace is as high as 1500 °C, which is at a high energy level. Even the thermal efficiency of water quenching method is near 60%, but the energy level difference of the process is up to 0.72 and exergy efficiency is only 12%. In other words, the available energy loses seriously in the water quenching process. Therefore, the fundamental way to improve slag sensible heat recovery efficiency is to reduce the energy level difference of the recycling process.

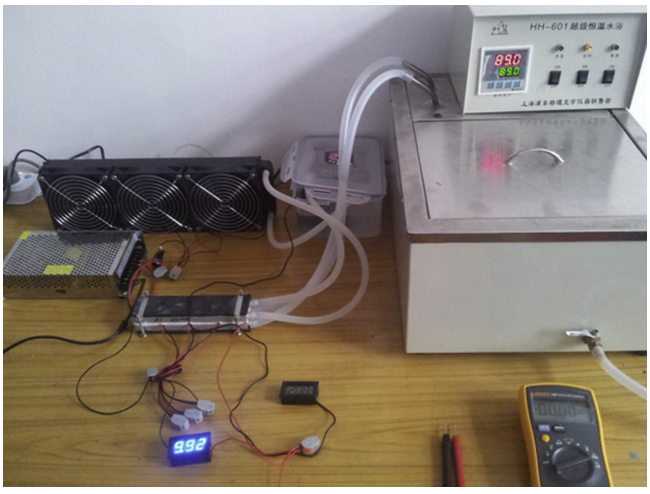

Fig. 17. The experimental thermoelectric power generation device driven by hot water.

The slag flushing water temperature does not exceed 100 °C at atmospheric pressure. If some organic solvent is added to the water which can increase the boiling point, the slag flushing water temperature can be improved. For example, adding a certain percentage of ethylene glycol can raise the boiling point of water to more than 150 °C, which can further improve the efficiency of power generation and reduce the cost recovery period. The calculations show that the power per square meter and efficiency can be increased to 2.4 kW/m^2 and 3.1%, respectively. The payback period can be reduced to 3–5 years. Of course, the cost of ethylene glycol, volatilization losses and the influence on the flashing effect should be considered in application.

Double working fluid power generation (low boiling point organic matter such as ethyl chloride acting working fluid) and thermoelectric power generation are the two main mature low-temperature power generation technologies below 100 °C. When the slag flushing water temperature is 100 °C, the efficiency of double working fluid power generation is 2–3% which is almost equal to the efficiency of thermoelectric power generation. The double working fluid power generation system is complex while thermoelectric power generation technology with modular features is easy to small-scale test operation and the maintenance costs is low. With the development of manufacturing technology of thermoelectric materials and modules, thermoelectric power generation technology is expected to be more advantageous.

A demonstration experimental device has been built, as shown in Fig. 17. The device consists of four power generation modules with dimensions of 40 × 40 × 4 mm^3. Hot water and cooling water inlet temperatures are 90.0 °C and 20.8 °C, respectively. The measured open-circuit voltage is 9.92 V, the short-circuit current is 821 mA, and the maximum power is 2.04 W. Furthermore one will improve this device mainly to add assembly for temperature and electrical signals in real time acquisition. It is expected to get more detailed experimental data and technical methods.

5. Conclusion

This study proposed a technical solution recycling blast furnace slag flashing water sensible heat based on thermoelectric power generation. Effects of some key parameters on the device performance are analyzed. The main conclusions are as follows:

(1) There is an optimal thermoelectric element length corresponding to the maximum power. Commercial thermoelectric module size meets the requirement for slag flushing water driven thermoelectric power generation.
(2) Enhancing the heat transfer between water and heat exchanger can effectively improve the power and efficiency of the device. For plate–fin heat exchanger, the power per square meter and efficiency are about 0.8 kW and 1.8%, respectively.
(3) When the thermoelectric element length matching the packing factor, the power reaches the maximum. Increasing the packing factor does not significantly improve the performance. The optimal packing factor is about 0.7.
(4) The too long flow path length leads to a low overall efficiency of the device. Improving the total power of the device can be achieved by increasing the number of heat exchanger channels and increasing the channel width.
(5) For blast furnace slag flushing water at 100 °C, water temperature drops 1.5 °C per meter, about 0.93 kW electrical energy can be produced per square meter area, and conversion efficiency of 2% can be achieved. The cost recovery period of the equipment is about 8 years.

Acknowledgments

This paper is supported by National Natural Science Foundation of China (No. 11305266) and National Basic Research Program of China (No. 2012CB720405). The authors wish to thank the reviewers for their careful, unbiased and constructive suggestions, which led to this revised manuscript.

References

[1] Guo ZC, Fu ZX. Current situation of energy consumption and measures taken for energy saving in the iron and steel industry in China. Energy 2010;35(11):4356–60.
[2] Ma G, Cai J, Zeng W, Dong H. Analytical research on waste heat recovery and utilization of China's iron & steel industry. Energy Proc 2012;14(2):1022–8.
[3] Zhang H, Dong L, Li H, Chen B, Tang Q, Fujita T. Investigation of the residual heat recovery and carbon emission mitigation potential in a Chinese steelmaking plant: a hybrid material/energy flow analysis case study. Sustain Energy Technol Assess 2013;2:67–80.
[4] Sun W, Cai J, Ye Z. Advances in energy conservation of China steel industry. Sci World J 2013;2013(1):8.
[5] Stijepovic MZ, Linke P. Optimal waste heat recovery and reuse in industrial zones. Energy 2011;36(7):4019–31.
[6] Ammar Y, Joyce S, Norman R, Wang Y, Roskilly AP. Low grade thermal energy sources and uses from the process industry in the UK. Appl Energy 2012;89(1):3–20.
[7] Gao C, Wang D, Dong H, Cai J, Zhu W, Du T. Optimization and evaluation of steel industry's water-use system. J Clean Prod 2011;19(1):64–9.
[8] Gao J, Li S, Zhang Y, Zhang Y, Chen P, Shen P. Process of re-resourcing of converter slag. J Iron Steel Res Int 2011;18(12):32–9.
[9] Goupil C, Seifert W, Zabrocki K, Uller EM, Snyder GJ, Snyder GJ. Thermodynamics of thermoelectric phenomena and applications. Entropy 2011;13:1481–517.
[10] Suzuki RO, Tanaka D. Mathematic simulation on thermoelectric power generation with cylindrical multi-tubes. J Power Sources 2003;122(2):201–9.
[11] Suzuki RO, Tanaka D. Mathematical simulation of thermoelectric power generation with the multi-panels. J Power Sources 2003;124(1):293–8.
[12] Suzuki RO. Mathematic simulation on power generation by roll cake type of thermoelectric double cylinders. J Power Sources 2004;124(1):293–8.
[13] Suzuki RO, Tanaka D. Mathematic simulation on power generation by roll cake type of thermoelectric tubes. J Power Sources 2004;133(2):277–85.
[14] Yu J, Zhao H. A numerical model for thermoelectric generator with the parallel-plate heat exchanger. J Power Sources 2007;172(1):428–34.
[15] Niu X, Yu J, Wang S. Experimental study on low-temperature waste heat thermoelectric generator. J Power Sources 2009;188(2):621–6.
[16] Astrain D, Vián JG, Martinez A, Rodriguez A. Study of the influence of heat exchangers' thermal resistances on a thermoelectric generation system. Energy 2010;35(2):602–10.
[17] Meng F, Chen L, Sun F. A numerical model and comparative investigation of a thermoelectric generator with multi-irreversibilities. Energy 2011;26(5):3513–22.
[18] Jang J, Tsai Y, Wu C. A study of 3-D numerical simulation and comparison with experimental results on turbulent flow of venting flue gas using thermoelectric generator modules and plate fin heat sink. Energy 2013;53:270–81.
[19] Lu H, Wu T, Bai S, Xu K, Huang Y, Gao W, et al. Experiment on thermal uniformity and pressure drop of exhaust heat exchanger for automotive thermoelectric generator. Energy 2013;54:372–7.
[20] Rowe DM, Min G. Evaluation of thermoelectric modules for power generation. J Power Sources 1998;73(2):193–8.
[21] Bejan A. Advanced engineering thermodynamics. 2nd ed. New York: Wiley; 1997.
[22] Qiu K, Hayden ACS. Development of a thermoelectric self-powered residential heating system. J Power Sources 2008;180(2):884–9.
[23] Lesage FJ, Potvin N. Experimental analysis of peak power output of a thermoelectric liquid-to-liquid generator under an increasing electrical load resistance. Energy Convers Manag 2013;66(1):98–105.
[24] Atik K. Thermoeconomic optimization in the design of thermoelectric cooler. Turkiye: Karabuk; 2009.
[25] Karthikeyan B, Kesavaram D, Ashok Kumar S, Srithar K. Exhaust energy recovery using thermoelectric power generation from a thermally insulated Diesel engine. Int J Green Energy 2012;10(10):1056–71.